Molecular and Phenotypic Analysis of 25 Recessive, Homozygous-Viable Alleles at the Mouse *agouti* Locus

Rosalynn J. Miltenberger,*,† Kazumasa Wakamatsu,‡ Shosuke Ito,‡ Richard P. Woychik,*,[1] Liane B. Russell* and Edward J. Michaud*,†,[2]

**Life Sciences Division, Oak Ridge National Laboratory, Oak Ridge, Tennessee 37831, †School of Genome Science and Technology, University of Tennessee, Knoxville, Tennessee 37996 and ‡Department of Chemistry, Fujita Health University School of Health Sciences, Toyoake, Aichi, 470-1192, Japan*

Manuscript received September 5, 2001
Accepted for publication November 8, 2001

ABSTRACT

Agouti is a paracrine-acting, transient antagonist of melanocortin 1 receptors that specifies the subapical band of yellow on otherwise black hairs of the wild-type coat. To better understand both agouti structure/function and the germline damage caused by chemicals and radiation, an allelic series of 25 recessive, homozygous-viable *agouti* mutations generated in specific-locus tests were characterized. Visual inspection of fur, augmented by quantifiable chemical analysis of hair melanins, suggested four phenotypic categories (mild, moderate, umbrous-like, severe) for the 18 hypomorphs and a single category for the 7 amorphs (null). Molecular analysis indicated protein-coding alterations in 8 hypomorphs and 6 amorphs, with mild-moderate phenotypes correlating with signal peptide or basic domain mutations, and more devastating phenotypes resulting from C-terminal lesions. Ten hypomorphs and one null demonstrated wild-type coding potential, suggesting that they contain mutations elsewhere in the ≥125-kb *agouti* locus that either reduce the level or alter the temporal/spatial distribution of *agouti* transcripts. Beyond the notable contributions to the field of mouse germ cell mutagenesis, analysis of this allelic series illustrates that complete abrogation of agouti function *in vivo* occurs most often through protein-coding lesions, whereas partial loss of function occurs slightly more frequently at the level of gene expression control.

In mice, as in many other mammals, the wild-type pigmentation pattern of the fur is called agouti. Individual hairs of an agouti coat are black, with a narrow ring of yellow pigment just below the tip; this alternative synthesis of eumelanin (black-brown pigments) *vs.* pheomelanin (yellow-red pigments) is regulated in a paracrine manner by the *agouti* locus in mice (Bultman *et al.* 1992). A short pulse of *agouti* expression at days 3–5 during the hair-growth cycle (Bultman *et al.* 1992) leads to a controlled wave of agouti protein secretion from the dermal papillae (Millar *et al.* 1995; Matsunaga *et al.* 2000). At nearby hair-bulb melanocytes, the agouti protein binds the melanocortin 1 receptor (Mc1r), thereby inhibiting binding by the agonist, α-melanocyte stimulating hormone (α-MSH; reviewed in Dinulescu and Cone 2000). Signaling by α-MSH through Mc1r promotes eumelanin synthesis, whereas agouti binding to Mc1r downregulates this signaling cascade and induces a transient switch from eumelanin to pheomelanin synthesis within hair-bulb melanocytes. Thus, recessive mutations at the *agouti* (*a*) locus, which impair agouti protein activity or reduce the level of *agouti* mRNA synthesis, result in a darker, less-yellow coat due to reduced pheomelanin banding of individual hairs. Conversely, dominant mutations, in which deregulated *agouti* mRNA synthesis leads to greater than normal agouti activity in the skin, give rise to increased yellow pigmentation of the fur. Most dominant *agouti* mutations produce ectopic agouti in tissues additional to the skin, resulting in a pleiotropic, maturity-onset obesity syndrome that is largely due to constitutive antagonism of related melanocortin receptors (Mcrs) in the central nervous system/hypothalamus (Bultman *et al.* 1992; Lu *et al.* 1994; Michaud *et al.* 1994a; Huszar *et al.* 1997; Ollmann *et al.* 1997). Facilitating agouti-mediated signaling through Mcrs in the skin and brain (Miller *et al.* 1997; Gunn *et al.* 1999; Nagle *et al.* 1999) are two other genes, *mahogany* and *mahoganoid*. Although the cellular function of *mahoganoid* is currently unknown, recent evidence suggests that mahogany is a low-affinity receptor for agouti on the surface of melanocytes (He *et al.* 2001).

Five protein structural domains are shared among the highly conserved mammalian homologs of *agouti* (Kwon *et al.* 1994; Leeb *et al.* 2000). Biological function of the various domains has been ascribed largely through analysis of mutations in the 131-amino-acid (aa) mouse agouti protein *in vivo* and through melano-

[1] *Present address:* Lynx Therapeutics, 25861 Industrial Blvd., Hayward, CA 94545.

[2] *Corresponding author:* Functional Genomics Group, Oak Ridge National Laboratory, Bldg. 1061, MS 6445, P.O. Box 2008, Oak Ridge, TN 37831-6445. E-mail: michaudejiii@ornl.gov

cortin (Mc) binding inhibition assays *in vitro*. The N-terminal 22 aa comprise a cleavable signal peptide that is indispensable *in vivo* (Hustad *et al.* 1995; Perry *et al.* 1996), as it provides entry into the secretory pathway (Blobel and Dobberstein 1975). The cysteine-rich C terminus (40 aa), which is believed to form a highly ordered, disulfide-bonded structure (Pallaghy *et al.* 1994), is both necessary and sufficient for Mc-binding inhibition at Mcrs *in vitro* (Willard *et al.* 1995; Kiefer *et al.* 1997), suggesting that the C-terminal domain binds directly to Mcrs *in vivo*. The mature agouti N terminus (34 aa) contains a conserved and presumably glycosylated arginine that is important for optimal activity *in vivo* (Perry *et al.* 1996). Similarly, the central, 29-aa basic domain is also required for full activity *in vivo* (Perry *et al.* 1996; Miltenberger *et al.* 1999). Although the biological role(s) of these domains remain uncertain, the mature N terminus and/or basic domain may mediate a low-affinity interaction with mahogany on the surface of melanocytes (He *et al.* 2001) and potentially promote a high-affinity interaction between the C terminus and adjacent Mc1rs. Sandwiched between the basic domain and the cysteine-rich region are several proline residues that contribute mildly to Mcr affinity and selectivity for the agouti protein *in vitro* (Kiefer *et al.* 1997). The prolines may provide a flexible "hinge" between the cysteine-rich C terminus and the rest of the protein, thereby better accommodating the possibly disparate protein-protein interactions mediated by these two portions of agouti *in vivo*.

To investigate further agouti structure/function relationships within its native context (*i.e.*, when synthesized from its normal chromosomal location and acting at its normal target, the hair-bulb melanocyte), we have characterized an allelic series of germline-induced, homozygous-viable, and recessive mutations, using both phenotypic and molecular tools. The 25 alleles analyzed here represent a relatively high percentage of all *a*-locus mutations that have been recovered in the morphological specific-locus test (SLT) at the Oak Ridge National Laboratory (ORNL) over several decades (Russell 1951, 2002). The mutant mice exhibit either hypomorphic (reduced function) or amorphic (no function) phenotypes ranging from extremely mild to null, with 56% (8 of the 18 hypomorphs, 6 of the 7 amorphs) encoding aberrant agouti proteins and 44% (10 hypomorphs, 1 amorph) being apparent regulatory mutations. The severity of associated phenotypes indicated the degree to which agouti activity was inhibited at the cellular level, and the visual interpretation of coat phenotypes was verified with a quantitative, chemical analysis of fur melanins. In addition to these data specific to *agouti* function, correlating the types of heritable DNA damage with various chemicals and radiation utilized in SLTs significantly augments growing toxicological databases and our current understanding of the mutability of mammalian germ cells.

MATERIALS AND METHODS

Mice: All mice originated and were maintained at the Oak Ridge National Laboratory and were fed Purina Laboratory Chow. The C3H/Rl (*A/A*), 101/Rl (A^w/A^w), and C57BL/10Rl (*a/a*) strains have been maintained by brother-sister inbreeding for >100 generations. All *a*-locus alleles analyzed arose in SLTs in which (101/Rl × C3H/Rl)F_1, and rarely (C3H/Rl × 101/Rl)F_1, males or females were treated with a mutagen (or were used as untreated controls; see Table 1) and then bred at selected intervals to noninbred T-stock females that were homozygous for recessive alleles (*a*, $Tyrp1^b$, $Tyr^{c\text{-}ch}$, *p*, $Myo5a^d$, Bmp^{se}, $Ednrb^s$) at seven visibly marked loci (Russell 1951). The *a*-locus mutations (A^w*, *A**) were therefore originally recovered as G_1 progeny (A^w*/*a*, *A**/*a*) carrying one copy of the severe regulatory allele, *nonagouti* (Bultman *et al.* 1992). Recessive *agouti* mutations were identified visually on the basis of reduced pheomelanin in the coat compared to nonmutated, agouti-pigmented littermates (A^w/a, *A/a*). Because *nonagouti* is dominant to null alleles, G_1 progeny carrying new amorphic mutations resembled homozygous *a/a* mice (black dorsal and ventral fur except for a few yellow-pigmented hairs on and behind the ears and around the perineum and mammae). In contrast, hypomorphs are dominant to *a*, and the primary hypomorphic mutants displayed a range of phenotypes that were intermediate between wild-type agouti (A^w/A^w, *A/A*) and nonagouti. Presumed primary *a*-locus mutants were allelism tested (by crossing to a^e/a^e) and were subsequently recovered for propagation and additional genetic tests. Mice carrying hypomorphic alleles were outcrossed to C57BL/10Rl for six or more generations to segregate away induced mutations at other loci and then intercrossed to determine homozygous viability and phenotype. Homozygous, hypomorphic phenotypes for each allele were generally less severe (more yellow) than in mice heterozygous for the same allele (A^w*/*a*, *A**/*a*). Primary mutants that appeared nonagouti were outcrossed to (101/Rl × C3H/Rl)F_1, and 12 homozygous lines (A^w*/A^w*, *A**/*A**, or the marker *a/a*) were established, revealing whether the mutation was amorphic or *a*-like. Amorphic *a*-locus mutations were identified by having uniformly "jet-black" fur, even in areas where nonagouti mice show some pheomelanin. Because all the alleles selected for this study were homozygous-viable (to exclude multi-locus mutagenic events), all were originally propagated as *a*-locus homozygous stocks. Despite avoidance of brother-sister matings, the small size of the stocks eventually caused decline in vigor in some of them, and six stocks were subsequently bred to be congenic with C57BL/10Rl, yielding *a*-locus heterozygotes (Table 1). One of these (a^{2R}) was successfully restored to homozygous breeding status. Although the 20 *a*-locus-homozygous stocks do not have identical genetic backgrounds, all of the hypomorphs have considerable contribution from C57BL/10Rl (due to the initial six or more outcrosses), and those propagating amorphs contain 101/Rl and C3H/Rl contributions.

Chemical analysis of melanins: Hair melanins were analyzed by direct chemical degradation of small hair samples, as described previously (Ito and Fujita 1985; Ozeki *et al.* 1995). The method is based on the formation of the specific degradation products, aminohydroxyphenylalanine (AHP) from pheomelanin and pyrrole-2,3,5-tricarboxylic acid (PTCA) from eumelanin. Ten to 20 mg of hair was homogenized in water (10 mg hair/ml), using a Ten-Brocke glass homogenizer. Hydrolysis of the hair with hydriodic acid produced AHP (yield 20%) that was then quantified by HPLC with electrochemical detection. Permanganate oxidation of hair samples produced PTCA (yield 2%) that was quantified by HPLC with UV detection. Due to the consistent yield of these degradation products, 1 ng AHP/mg hair corresponds to 5 ng pheomelanin/mg hair.

Likewise, 1 ng PTCA/mg hair corresponds to 50 ng eumelanin/mg hair. Four to six hair samples were plucked from the dorsal midline of a single animal for each allele. Analysis of variance with a 95% confidence level determined that the variance was not equal; therefore, data were analyzed using a two-sample Student's *t*-test, assuming equal variance.

RNA preparation: Total RNA was prepared from the skin of 4-day-old neonatal mice using standard guanidine isothiocyanate procedures (Ausubel *et al.* 1989) or the rapid total RNA isolation kit (5 Prime → 3 Prime). Skin was obtained from the dorsal and/or ventral body region, excluding the head, legs, and tail. For homozygous mutant mice, up to three neonates were used per RNA preparation. For mutant stocks maintained as heterozygotes, no fewer than five neonates were used since the phenotype of a^R/a and a/a littermates was not readily apparent at day 4. In the case of a^{6R}, however, a single heterozygous a^{6R}/a neonate was analyzed from an outcross between a homozygous mutant and C57BL/10Rl mate.

RT-PCR analysis: Total RNA (2 μg) derived from dorsal and ventral skin was reverse transcribed using random hexamer primers (Pharmacia, Piscataway, NJ) and MMLV-reverse transcriptase (Promega, Madison, WI). The RT-PCR products in Figure 3 were obtained by using 1 μl of ventral skin cDNA and one of two forward primers (exon 1A-specific 5′-CACCAG TCTGAGTCCTTGAGCC-3′; exon 2-specifc 5′-GACGCTTGGA GATGACAGGAGTCTG-3′) with a common reverse primer (exon 4-specific 5′-AAACGGCACTGGCAGGAGGC-3′). The entire *agouti* coding region was amplified by PCR using 1–10 μl of dorsal and ventral skin cDNA and primers specific for the very 5′ end of exon 2 (5′-GCTTCTCAGGATGGATGTCA-3′) and the untranslated region of exon 4 (5′-CAATCACCCGTT CCCGAAGC-3′). The PCR products were cloned into the TA vector (Invitrogen, San Diego) and multiple, individual clones were sequenced for each mutant allele.

Northern analysis: Selection of poly(A)$^+$ mRNA was performed using the Oligotex mRNA mini kit (QIAGEN, Valencia, CA) and total RNA (250 μg) derived from dorsal neonatal skin. For a^{6R}, RNA was derived from the whole skin of a single a^{6R}/a neonate, rather than from the dorsal skin only. A Northern blot made by formaldehyde agarose gel electrophoresis was hybridized with a ^{32}P-labeled *agouti* cDNA probe (Church and Gilbert 1984; Sambrook *et al.* 1989) and exposed to a phosphorimager (Fujix BAS system; Fuji, Stamford, CT) plate overnight to quantify the intensity of the *agouti* band and then to X-ray film for 3 days. The blot was subsequently hybridized with a low specific-activity probe for *Gapdh* and exposed to a phosphorimager plate 4 hr for quantification and then to X-ray film overnight.

Genomic DNA analysis: Genomic DNA was obtained from tail biopsy and Southern analysis was performed using standard procedures (Church and Gilbert 1984; Sambrook *et al.* 1989). Individual exons of *agouti* including splice junctions were amplified by PCR using the following primers: exon 2 forward (5′-ATCCCTTACCACCATCTTCT-3′) and reverse (5′-AGGAAGCACCATAGCTCTG-3′); exon 3 forward (5′-CTGGCTT TGCTCCTTTCT-3′) and reverse (5′-GTTTCCTGGAGGCCAGG AAG-3′); exon 4 forward (5′-AGAGGTCTCTGTCCTGACCT-3′) and the reverse primer described above that binds within the untranslated region of exon 4. The entire ~5.5-kb genomic region containing all three coding exons was amplified using the Expand Long Template PCR system (Boehringer Mannheim, Indianapolis) and the exon 2 forward and exon 4 reverse primers just described. To amplify the remainder of the 3′ untranslated region (310 bp total) that was not included in previous RT-PCR or genomic clones and that includes the poly(A) signal, the forward primer 5′-GCTTCGGGAACGGGTGA TTG-3′ and reverse primer 5′-TTTCCCTATGCAAGAGTGGC-3′ were used. The hair cycle-specific promoter region and 5′ untranslated exons 1B and 1C (715 bp total) were amplified using the forward primer 5′-GGAGAGCCGCAGCCTAATCC-3′ and reverse primer 5′-CTGAAAGGGAACCATACAGA-3′. All PCR products were then cloned into the TA or TOPO TA vectors (Invitrogen) and multiple individual clones were sequenced.

DNA sequence analysis: DNA samples from individual clones were sequenced using the ABI dye terminator ready reaction mix (Perkin-Elmer, Norwalk, CT) or the Big Dye terminator sequencing kit (Perkin-Elmer) and an ABI 377 automated DNA sequencer. The DNA sequence was then analyzed using the following software: Sequence Navigator (version 1.0.0; Applied Biosystems, Foster City, CA), Factura (version 1.2.0r6; Applied Biosystems), Auto Assembler (version 1.4.0; Applied Biosystems), and MacVector (version 6.5; Oxford Molecular, Palo Alto, CA).

RESULTS

Phenotypic analysis: Eighteen hypomorphic alleles were grouped into four phenotypic categories (see below) according to the amount of pheomelanin reduction that is visually apparent in the hair, with primary weight given to the appearance of fur along the dorsal midline. Seven alleles with jet-black fur comprised a separate, fifth group. Individual alleles are listed in Table 1, each designated by its superscript symbol. The order of hypomorphic alleles (a^{1R} through a^{18R}), both between and within the four phenotypic categories, corresponds to the severity of coat phenotypes in adult mice of the indicated genotype (note that some are heterozygotes; see MATERIALS AND METHODS). The mutagens employed, year when each allele was originally identified, and original ORNL stock designation are also shown. The germ-cell stage in which each mutation arose is indicated also, on the basis of the interval between mutagen exposure and conception of the mutant and utilizing existing germ-cell development data (Oakberg 1984).

Figure 1 shows representative homozygous mutant mice from each phenotypic group compared with a wild-type agouti mouse in each panel. Mild hypomorphs exhibit a subtle diminution in adult dorsal fur pheomelanin compared to the wild-type agouti strains of origin C3H/Rl (A/A) or 101/Rl (A^w/A^w). Other body regions, such as the sides and ventrum, are not noticeably different from wild type. Moderate hypomorphs comprise the largest phenotype group in which the darkened agouti coat displays reduced pheomelanin in all body regions, although the effect is generally more apparent in dorsal fur. The third category (umbrous-like) is unusual due to preferential darkening of fur along the dorsal midline from nose to tail. In the ventrum and at the dorsal/ventral boundary, however, nearly wild-type levels of yellow-banded fur are apparent, with gradual attenuation in pheomelanin along the sides of the animal toward the dorsal midline. Severe *agouti* hypomorphs exhibit an obvious reduction in fur pheomelanin in all body regions such that the fur appears very dark but not

TABLE 1

Phenotype and generation of recessive *agouti* mutations

Phenotype group	Mutation	Stock name	Genotype	Mutagen	Germ-cell stage	Date	Note
Mild[a]	1R	37R145L	a^{1R}/a^{1R}	Neutrons	SG	1965	
	2R	1FAFye	a^{2R}/a^{2R}	X rays	Oocytes	1965	
	3R	4MNURh	a^{3R}/a	MNU	DG	1982	
Moderate[b]	4R	4DThWb	a^{4R}/a^{4R}	Spontaneous	NA	1966	2
	5R	66CoS	a^{5R}/a^{5R}	γ rays	SG	<1984	1
	6R	3THO-IV	a^{6R}/a	Tritiated H_2O	SG	1975	
	7R	12SYNg	a^{7R}/a	Synthetic fuel	SG	1979	
	8R	76G	a^{8R}/a^{8R}	X rays	EST	1956	1
	9R	120ENURd	a^{9R}/a^{9R}	ENU	SG	1980	1
	10R	9ETOc	a^{10R}/a^{10R}	Ethylene oxide	SG	1983	
	11R	9R75H	a^{11R}/a^{11R}	Neutrons	SG	1964	1
Umbrous-like[c]	12R	4FrSb	a^{12R}/a	γ rays	SG	1963	
	13R	55UTh	a^{13R}/a^{13R}	γ rays	SG	1960	
	14R	75ENURd	a^{14R}/a^{14R}	ENU	SG	1980	
	15R	111ENURd	a^{15R}/a^{15R}	ENU	SG	1979	
Severe[d]	16R	14R75VH	a^{16R}/a^{16R}	Neutrons	SG	1965	2
	17R	58DSD	a^{17R}/a^{17R}	X rays	SG	1963	
	18R	48DTD	a^{18R}/a	X rays	SG	1962	
Null[e]	19R	23ENURhh	a^{19R}/a^{19R}	ENU	SG	1985	3
	20R	9ENURh	a^{20R}/a^{20R}	ENU	SG	1980	
	21R	5FrSb	a^{21R}/a^{21R}	γ rays	SG	1963	
	22R	207G	a^{22R}/a^{22R}	Spontaneous	NA	1957	
	23R	14DTTMb	a^{23R}/a^{23R}	X rays	SG	1986	
	24R	11DT	a^{24R}/a^{24R}	X rays	SG	1959	
	25R	15CoS	a^{25R}/a^{25R}	γ rays	SG	1958	

Phenotypes are based on the appearance of coats in adult mice ~8 weeks of age of the indicated genotypes. MNU, *N*-methyl-*N*-nitrosourea; ENU, *N*-ethyl-*N*-nitrosourea; EMS, ethyl methanesulfonate; SG, stem cell spermatogonia; DG, differentiating spermatogonia; NA, not applicable; EST, early spermatid; Note 1, prominent demarcation at the dorsal/ventral boundary, as in 101/R1 strain; Note 2, phenotype among littermates is variable; however, the mildest phenotype is indicated; Note 3, nearly null phenotype with pheomelanin present around nipples and perineum.

[a] Banded hairs are present in the dorsum, sides, and ventrum, with pheomelanic hair around nipples, perineum, and behind ears.

[b] Banded hairs are present in all body regions, but with reduced pheomelanin. Dorsum is moderately darker than the sides of ventrum. Pheomelanin is prominent around nipples, perineum, and behind ears.

[c] Pheomelanin is severely reduced along dorsal midline. Banded hair is present on the sides and ventrum but with reduced pheomelanin. Pheomelanin is also reduced around nipples, perineum, and behind ears.

[d] Pheomelanin is severely reduced in dorsum, sides, and ventrum and moderately reduced around nipples, perineum, and behind ears.

[e] Hairs are completely eumelanic with no pheomelanin banding. No pheomelanin is present around nipples, perineum, and behind ears. Exception is noted for the nearly null allele, a^{19R} (see Note 3).

completely black. The fur of homozygous null *agouti* mice is entirely black, even in areas where nonagouti mice typically display a few yellow hairs (ears, perineum, and mammae). The single exception in this category is a^{19R}, which is not a true null, as it displays some yellow pigmentation around the mammae and perineum, but no yellow hairs on or behind the ears (or in any other region).

To augment visual description of these mutant phenotypes and to gain a quantifiable measure of *agouti* gene loss of function, we directly analyzed the amount of pheomelanin and eumelanin in the fur of recessive *agouti* alleles. In this relatively simple yet sensitive procedure (Ito and Fujita 1985; Ozeki *et al.* 1995; Ito 1998), chemical treatment of small fur samples yields specific degradation products that are readily detectable by HPLC. The amount of AHP isomers and PTCA is directly proportional to the amount of pheomelanin and eumelanin, respectively, in the original fur sample. This type of analysis has been useful in determining even subtle variations in the distribution of hair melanins induced by various coat color mutations in the mouse (Gunn *et al.* 2001; Lamoreux *et al.* 2001).

Figure 2 shows the chemical analysis of melanins from dorsal midline fur of adult *agouti* mutant mice. AHP

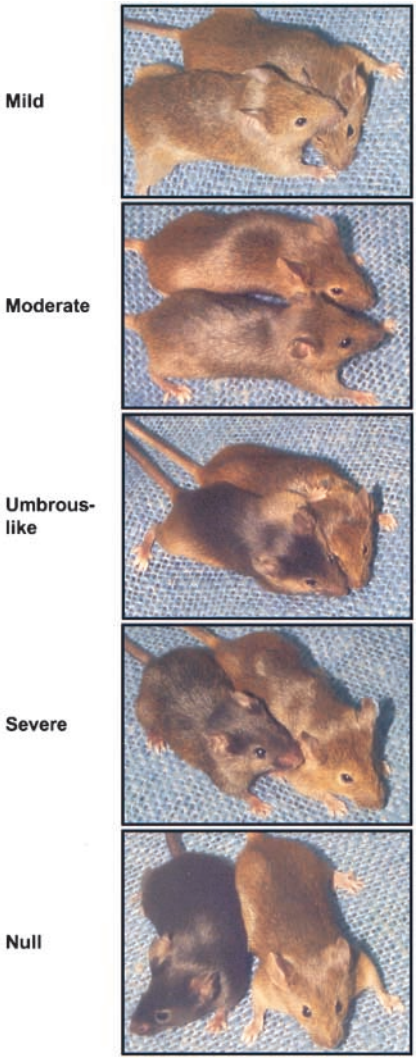

FIGURE 1.—Coat-color phenotypes of recessive *agouti* mutations. Representative mice from each mutant category are shown, from the mildest category (mild) at the top to the most severe (null) at the bottom. A wild-type mouse (101/Rl; A^w/A^w) is shown above or to the right of the mutant in each photo. The specific alleles used from each phenotypic category are as follows: mild, a^{1R}; moderate, a^{11R}; umbrous-like, a^{13R}; severe, a^{17R}; null, a^{21R}. All mice were 8 weeks of age and homozygous for the mutant or wild-type alleles.

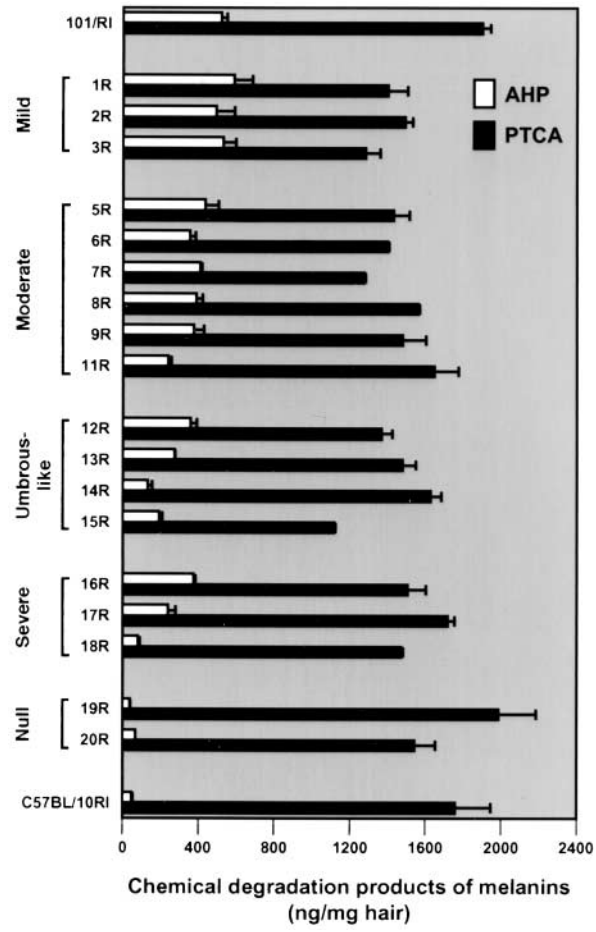

FIGURE 2.—Chemical analysis of hair pigments. AHP (derived from pheomelanin) and PTCA (derived from eumelanin) are indicated by open and solid bars, respectively. Data represent mean AHP or PTCA values (nanograms per milligram of hair) analyzed from a single mouse for each allele. Error bars indicate the variation between separate AHP and PTCA measurements ($n \geq 2$) from a single chemical degradation experiment. Alleles analyzed are indicated on the *y*-axis and are grouped by phenotypic category, from mildest at the top to most severe (least amount of pheomelanin) at the bottom. The genotypes and ages of adult mice were as follows: 101/Rl (A^w/A^w), 22 weeks; a^{1R}/a^{1R}, 31 weeks; a^{2R}/a^{2R}, 26 weeks; a^{3R}/a, 21 weeks; a^{5R}/a^{5R}, 25 weeks; a^{6R}/a, 18 weeks; a^{7R}/a, 29 weeks; a^{8R}/a^{8R}, 24 weeks; a^{9R}/a^{9R}, 24 weeks; a^{11R}/a^{11R}, 25 weeks; a^{12R}/a, 18 weeks; a^{13R}/a^{13R}, 22 weeks; a^{14R}/a^{14R}, 18 weeks; a^{15R}/a^{15R}, 26 weeks; a^{16R}/a^{16R}, 27 weeks; a^{17R}/a^{17R}, 28 weeks; a^{18R}/a, 26 weeks; a^{19R}/a^{19R}, 22 weeks; a^{20R}/a^{20R}, 31 weeks; and C57BL/10Rl (a/a), 22 weeks.

values varied over a 10-fold range and generally correlated with the severity of visual coat phenotypes in the alleles tested, although a few exceptions were noted (a^{12R}, a^{16R}, and a^{20R}). As a group, mild mutations contained about the same level (102%) of AHP in dorsal fur as did the wild-type control (101/Rl); moderate alleles contained 71%; umbrous-like, 46%; severe, 48%; nulls, 13%; and nonagouti (C57BL/10Rl), 9%. Mean AHP levels for individual mutations compared to the wild-type control were significantly lower ($P < 0.05$) for the darker mutations (nulls, nonagouti, and hypomorphs a^{11R}, a^{13R}, a^{14R}, a^{15R}, a^{16R}, a^{17R}, and a^{18R}), but not for the more temperate hypomorphs (a^{1R}, a^{2R}, a^{3R}, a^{5R} a^{6R}, a^{7R} a^{8R}, a^{9R}, and a^{12R}). Heterozygous status of five alleles (a^{3R}/a, a^{6R}/a, a^{7R}/a, a^{12R}/a, and a^{18R}/a) and mild heterogeneity in the genetic backgrounds of homozygous alleles did not alter the overall trend, nor did age variation among adult mice tested (18–31 weeks) contribute significantly to the variance in mean AHP or PTCA determinations, although age generally enhances the level of visible pheomelanin in the coat. With respect to PTCA levels, significant differences ($P < 0.05$) were observed for most alleles (except a^{19R}) compared to either the 101/Rl (wild type) or the C57BL/10Rl (nonagouti black) control;

however, the variation was <2-fold and did not follow a consistent trend with respect to the *agouti* allelic series. Slight heterogeneity in genetic background among the various mutant stocks could explain this low yet significant variation in eumelanin content. Altogether, these data demonstrate a fair (albeit imperfect) correlation between chemically determined pheomelanin content and visual determination of the severity of *agouti* loss of function in the various alleles, suggesting that this method provides a semiquantitative measure of the effect of *agouti* mutations on the level of pheomelanin synthesis *in vivo*.

Molecular analysis: The 25 recessive alleles were generated in (101/Rl × C3H/Rl)F_1 hybrid mice (see MATERIALS AND METHODS), so the mutations arose on either a C3H/Rl (*A*) or a 101/Rl (A^w) chromosome. The wild-type, parental alleles *A* and A^w differentially express four alternatively spliced transcripts (BULTMAN *et al.* 1992, 1994; VRIELING *et al.* 1994) that encode a common protein sequence (Figure 3A). Whereas both *A* and A^w express the temporally restricted transcripts that give rise to the characteristic subapical band of pheomelanin in dorsal and ventral hairs, only A^w expresses the ventral-specific transcripts that uniquely generate a predominantly yellow or cream-colored ventrum in A^w-derived alleles. To determine the parental allele of origin for the 25 recessive mutations, and to help explain ventral fur phenotypes among the various alleles, we employed a reverse transcriptase-polymerase chain reaction (RT-PCR) strategy using ventral skin from neonatal mice and two PCR primer sets (Figure 3B). One set of primers (Ex 2–4) amplified the coding region that is common to all transcripts in both *A*- and A^w-derived alleles. The other set (Ex 1A–4) is unique to ventral-specific transcripts in A^w-derived alleles only and yields a larger-sized product. Findings from this analysis were then confirmed by Southern analysis (CHEN *et al.* 1996) using an Exon 1A′-specific probe (data not shown). As summarized in Table 2, 11 hypomorphic and 4 amorphic alleles arose on the C3H/Rl (*A*) chromosome, whereas 7 hypomorphs and 3 amorphs were derived from 101/Rl (A^w). Although each of the smaller phenotype groups contained exclusively *A*- or A^w-derived alleles, the distribution appeared random in the larger phenotypic categories (moderate, null), suggesting no significant correlation between phenotype category and parental allele mutated.

To identify the precise nature of DNA damage that produced the *agouti* coat phenoytpes, we analyzed the *agouti* locus at both the genomic and mRNA expression levels. The entire coding region (exons 2–4) of *agouti* was amplified by RT-PCR from both dorsal and ventral skin of neonatal mice carrying each mutant allele (data not shown; see MATERIALS AND METHODS). The RT-PCR products were cloned, and several clones from each allele were sequenced to identify potential mutations within the *agouti* protein-coding region. The affected exon(s) were then isolated from genomic DNA of the appropriate mutant by PCR, cloned, and sequenced to verify the initial RT-PCR results. Further independent verification of these sequence alterations was gained through RNase protection assay, using the entire *agouti* coding region as a probe (data not shown). Table 2 summarizes the results of these molecular analyses.

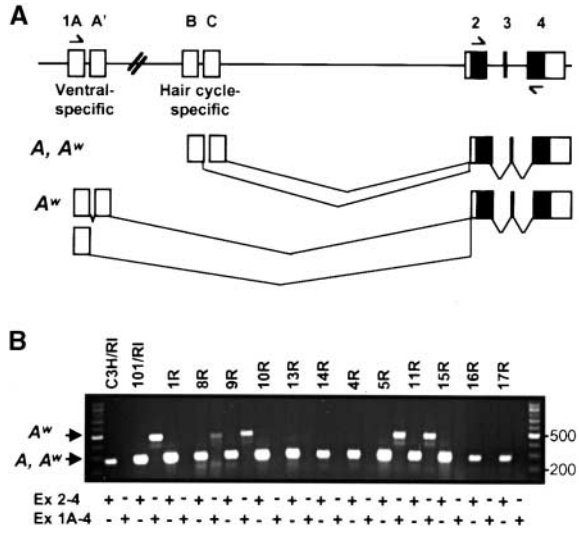

FIGURE 3.—Schematic of the *agouti* gene and RT-PCR analysis. (A) Alternative promoters drive expression of multiple *agouti* isoforms in wild-type skin. The horizontal line represents genomic DNA spanning ~125 kb at the *agouti* locus and the boxes represent exons (not drawn to scale). Noncoding exons (1A, 1A′, 1B, 1C, and parts of 2 and 4) are indicated by open boxes. Solid boxes represent protein-coding exons (2–4). In B, primers used for RT-PCR analysis are indicated by arrows (above exons 1A and 2; below exon 4). Two promoter regions (ventral-specific and hair cycle-specific) are separated by ~100 kb, as indicated by a break in the line. Each promoter utilizes two sets of alternative 5′ exons that splice into the same set of coding exons, as indicated by V-shaped lines joining the exons. In mice carrying either the *A* (C3H/Rl) or the A^w (101/Rl) allele, the hair cycle-specific promoter utilizes two transcription initiation sites (at 1B or 1C), yielding two transcripts of approximately the same size in both the dorsal and ventral skin. In mice carrying the A^w allele, a single transcription initiation event (at 1A) from the ventral-specific promoter produces two alternative transcripts, which differ by the inclusion or exclusion of exon 1A′. (B) RT-PCR analysis of *agouti* transcripts in wild-type and representative mutant alleles. Mutant alleles are indicated by their superscript symbol (*e.g.*, 1R for a^{1R}). Two primer sets, indicated by Ex 2–4 or Ex 1A–4 at the bottom, were used to amplify differentially expressed *agouti* transcripts. All PCR reactions were performed simultaneously from reverse-transcribed RNA prepared from the ventral skin of 4-day-old homozygous neonatal mice. To the left, the arrow labeled *A*, A^w marks the exon 2–4 product (267 bp) that is present in mutants derived from either a parental *A* (C3H/Rl) or a A^w (101/Rl) allele. The arrow labeled A^w indicates the exon 1A–4 products (492 or 446 bp) that are unique to A^w-derived alleles. DNA size standards (100-bp ladder) are shown in the first and last lanes, with the 200 and 500 bp bands indicated on the right.

Of the 25 recessive alleles characterized, 14 alleles with phenotypes ranging from mild to null demonstrated aberrant protein-coding potential. Point muta-

TABLE 2

Summary of the molecular characterization of recessive *agouti* mutations

Phenotype group	Genotype	Parental allele	DNA change	Amino acid change	mRNA level[a]	Site/type of lesion
Mild	a^{1R}/a^{1R}	*A*	TGA → TTA	stop → Leu_{132} + 26 aa	~Wt	E4-cysteine-rich domain
	a^{2R}/a^{2R}	*A*	None identified[b]	None	ND[c]	Regulatory
	a^{3R}/a	*A*	GAA → AAA	Glu_{66} → Lys	ND[c]	E3-basic domain
Moderate	a^{4R}/a^{4R}	*A*	None identified	None	↓4.0×	↓ mRNA levels
	a^{5R}/a^{5R}	A^w	None identified	None	↓4.5×	↓ mRNA levels
	a^{6R}/a	*A*	None identified	None	↓3.8×[d]	↓ mRNA levels
	a^{7R}/a	*A*	None identified	None	ND[c]	Regulatory
	a^{8R}/a^{8R}	A^w	Δ 9 nt	Δ $Phe_{14}Leu_{15}Cys_{16}$	~Wt	E2-signal peptide
	a^{9R}/a^{9R}	A^w	GTC → GAC	Val_3 → Asp	~Wt	E2-signal peptide
	a^{10R}/a^{10R}	*A*	AG → TG	Δ $Lys_{76}Lys_{77}$	↓2.9×	E4-splice acceptor, basic domain
	a^{11R}/a^{11R}	A^w	None identified	None	~Wt	Regulatory/cell type
Umbrous-like	a^{12R}/a	*A*	GCC GAG → GCA AAG[b]	Glu_{68} → Lys	ND[c]	E3-basic domain
	a^{13R}/a^{13R}	*A*	GAG → AAG	Glu_{68} → Lys	~Wt	E3-basic domain
	a^{14R}/a^{14R}	*A*	TCC → CCC	Ser_{112} → Pro	~Wt	E4-cysteine-rich domain
	a^{15R}/a^{15R}	*A*	None identified	None	~Wt	Regulatory/cell type
Severe	a^{16R}/a^{16R}	A^w	None identified	None	↓2.7×	↓ mRNA levels
	a^{17R}/a^{17R}	A^w	None identified	None	↓3.6×	↓ mRNA levels
	a^{18R}/a	A^w	None identified	None	ND[c]	Regulatory
Null	a^{19R}/a^{19R}	*A*	TGC → AGC	Cys_{115} → Ser	~Wt	E4-cysteine-rich domain
	a^{20R}/a^{20R}	A^w	TGC → TGA	Cys_{110} → stop	~Wt	E4-cysteine-rich domain
	a^{21R}/a^{21R}	A^w	Δ 11 nt	Δ Phe_{118}-Ala_{121} + fs	~Wt	E4-cysteine-rich domain
	a^{22R}/a^{22R}	A^w	TTC → TCC	Phe_{118} → Ser	~Wt	E4-cysteine-rich domain
	a^{23R}/a^{23R}	*A*	Δ CTC → TA	Ser_{49} → Met + fs	↓4.0×	E2-N terminus, fs, premature termination
	a^{24R}/a^{24R}	*A*	None identified	None	ND	Regulatory
	a^{25R}/a^{25R}	*A*	Δ 359 nt	Δ Ala_{54} → Lys_{75} + fs	~Wt	E3, E4-Δ basic domain, fs, cysteine-rich domain
Controls	C3H/R1-*A/A*	—	None	None	Wt	Wild type
	101/R1-A^w/A^w	—	None	None	Wt	Wild type
	C57BL/10R1-*a/a*[e]	*A*	AGC → GGC	Ser_{13} → Gly	↓7.1×	↓ mRNA levels, E2-signal peptide

Affected nucleotides are indicated by the underlined nucleotides within the context of their codon triplet code. Δ, deletion; aa, amino acids; Wt, wild type; ↓, reduced; ND, not determined; E2, exon 2; E3, exon 3; E4, exon 4; fs.

[a] RNA was prepared from homozygous neonates, unless otherwise noted. Level of *agouti* mRNA expression was normalized to the level of *Gapdh* expression in each sample and then compared to the *Gapdh*-normalized value in C3H/R1 and 101/R1 mice. ~Wt indicates that the normalized expression levels in mutant alleles were ±20% of the normalized level in C3H/R1 and 101/R1 mice.

[b] DNA was obtained from homozygous mutant adults (a^{2R}/a^{2R}; a^{12R}/a^{12R}), as determined by breeding tests.

[c] When neonates were collected for RNA analysis, these stocks were maintained as heterozygotes. Because *agouti* expression occurs in neonates prior to a visible fur distinction between a^R/a and *a/a* (black, extremely low *agouti* expression) littermates, RNA was prepared from five neonates of mixed (a^R/a or *a/a*) genotype. Consequently, quantification of *agouti* RNA levels in these mutants is not directly comparable to other mutant or wild-type alleles.

[d] RNA was prepared from a^{6R}/a neonates only.

[e] C57BL/10R1 was included as the relevant heterozygote reference. The primary mutation in *nonagouti* is a severe regulatory defect (Bultman *et al.* 1992; Figure 4) that is common to both C57BL/6J and C57BL/10R1 inbred strains. C57BL/6J-*a/a* is like A^w at the ventral-specific promoter region (Bultman *et al.* 1994; Chen *et al.* 1996) and wild type in the protein-coding region, whereas C57BL/10R1-*a/a* carries the *A* orientation at the ventral-specific promoter and a novel signal peptide mutation.

tions and small intragenic deletions were found in several domains of the agouti protein that have been shown previously to be important for *agouti* function *in vivo* (Hustad *et al.* 1995; Perry *et al.* 1996; Miltenberger *et al.* 1999). Two mutations were identified in the signal peptide (a^{8R} and a^{9R}, moderate), four within the basic domain (a^{3R}, mild; a^{10R}, moderate; a^{12R} and a^{13R}, umbrous-like), and six in the cysteine-rich C terminus (a^{1R}, mild;

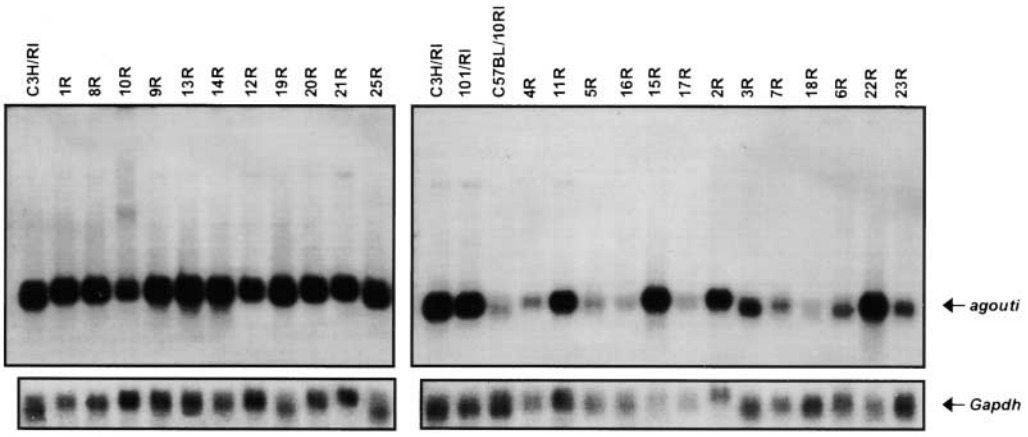

FIGURE 4.—Northern analysis. Each lane contains poly(A)+ mRNA (~2.5 μg) prepared from the dorsal skin of 4-day-old neonatal mice, whose superscript allele designation is indicated at the top (*e.g.*, 1R for a^{1R}). Arrows to the right indicate the *agouti*-specific band and the internal control, *Gapdh*. Left, gene expression in the C3H/Rl (*A/A*) control *vs.* alleles known to carry *agouti* protein-coding alterations. Right, gene expression in the C3H/Rl (*A/A*), 101/Rl (A^w/A^w), and C57BL/10Rl (*a/a*) controls *vs.* other alleles that carry either protein-coding or regulatory mutations. Homozygous mice were used where available. For the 6R allele, RNA was prepared from a single a^{6R}/a neonate. For all other heterozygous alleles (a^{2R}, a^{3R}, a^{7R}, a^{12R}, a^{18R}), RNA was prepared from an unknown mixture (a^R/a and *a/a*) of five or more neonates.

a^{14R} umbrous-like; a^{19R}, a^{20R}, a^{21R}, and a^{22R}, null). Two additional null alleles (a^{23R} and a^{25R}) contained deletions that induced reading-frame shifts and/or premature termination signals such that the protein sequence of the entire basic region and C terminus was either deleted or completely modified. Overall, these results indicate that lesions in the N-terminal and central regions of the agouti protein tend to generate hypomorphic phenotypes, whereas C-terminal alterations generally induce complete loss-of-function phenotypes.

In the remaining 11 alleles, several lines of evidence indicated that they have wild-type protein-coding potential, suggesting that these alleles probably contain mutations that affect proper regulation of *agouti* expression in the skin. Further sequence analysis was performed to examine the introns and splice junctions between exons 2 and 4, the 3′ noncoding sequence, the 5′ untranslated exons 1B and 1C, and several hundred base pairs around the hair cycle-specific promoter (Figure 3A). No DNA alterations were found in any of these regions of the 11 putative regulatory alleles, indicating that the lesions most likely lie elsewhere in the ≥125-kb *agouti* locus (VRIELING *et al.* 1994). The ventral-specific promoter and its adjacent 5′ untranslated exons were not analyzed in any of the mutants because the hypomorphic phenotypes were most evident in dorsal banded fur.

To ascertain whether the level of mRNA expression was altered in any of the mutant mice, Northern analysis was performed (Figure 4). Using *Gapdh* as a loading control, 5 of the 11 putative regulatory alleles (right side: a^{4R}, a^{5R}, and a^{6R}, moderate; a^{16R} and a^{17R}, severe) demonstrated diminished levels of steady-state *agouti* mRNA expression compared to either of the wild-type controls or to the previously characterized protein-coding mutations (the majority are in the left of Figure 4). However, one protein-coding mutation, a^{10R}, demonstrated slightly reduced levels of mRNA expression due to a splicing defect. A single-base change at the normal exon 4 splice-acceptor site prompts usage of a surrogate splice acceptor within the exon 4 coding region, which is apparently less efficient, as indicated by a larger RNA product in the a^{10R} lane. Northern analysis also indicated that 2 (a^{11R}, moderate; a^{15R}, umbrous-like) of the 11 putative regulatory alleles express normal to high levels of *agouti* message, which is wild type in sequence. In the case of alleles maintained as heterozygotes (a^{2R}, a^{3R}, a^{7R}, a^{12R}, and a^{18R}), quantification of RNA levels was not possible since a^R/a individuals could not be distinguished from *a/a* littermates. In addition, RNA analysis was not performed for the a^{24R} allele due to poor stock viability. However, extensive sequence analysis of genomic DNA from a^{24R} adults clearly indicated wild-type sequence in the protein-coding region, 3′ untranslated region, and ~1 kb surrounding the hair cycle-specific promoter and hair cycle-specific 5′ untranslated exons.

DISCUSSION

Agouti structure and function: One of the most challenging aspects of this study was accurate correlation of the severity of *agouti* mutant phenotypes with the molecular changes in the locus (summarized in Figure 5A). On the basis of earlier studies (BULTMAN *et al.* 1991; PERRY *et al.* 1996; KIEFER *et al.* 1997, 1998), we expected that the more severe mutations would map to the C-terminal region of agouti that is believed to bind Mcrs. In fact, all null mutations except one (a^{24R}) altered the coding potential of the C terminus and thus ablated *agouti* activity at the cellular level, although the a^{19R} allele was nearly null with respect to ventral pigmentation. The hypomorphic mutations, in contrast, mapped to various regions throughout the agouti protein or appeared to be regulatory in nature and generated a range of phenotypes, some of which were extremely subtle. Assortments of apparent regulatory mutations, point mutations, and small deletions were found in each phe-

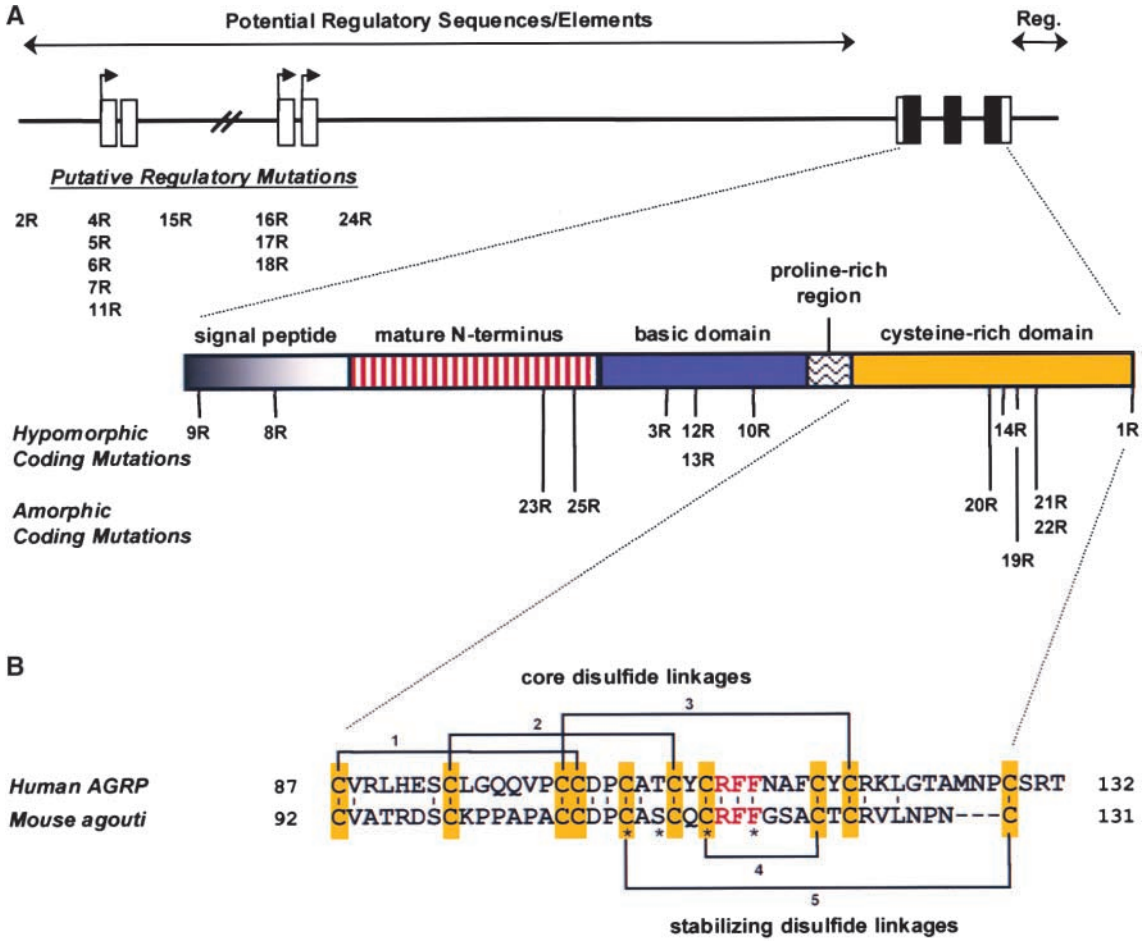

FIGURE 5.—Summary of molecular analysis. (A) Schematic of the ≥125-kb *agouti* locus. The thick horizontal line represents the genomic DNA, with solid boxes representing protein-coding exons, open boxes representing noncoding exons (not drawn to scale), and arrows above the noncoding exons representing transcriptional start sites. Two promoter regions are separated by ~100 kb, as indicated by a break in the line. Location of regulatory elements is postulated by the double-headed arrows above the gene, both 5′ (BULTMAN *et al.* 1992, 1994; VRIELING *et al.* 1994) and 3′ (MILLER *et al.* 1994) to the coding exons. Specific alleles believed to carry regulatory mutations are indicated at left, beneath the transcriptional promoters. Allele designations (*e.g.*, 2R for a^{2R}) for the presumed regulatory mutations are aligned in columns that refer to the phenotype categories, from the mildest at the left to the most severe at the right. Dotted lines extending downward from the coding exons show an expanded view of the agouti protein, with the various structural domains indicated. The positions of hypomorphic (1R–14R) and amorphic (19R–25R) coding mutations are indicated below the protein schematic. The position of the 25R mutation also corresponds to the exon 2/3 boundary, and the 10R mutation corresponds to the exon 3/4 boundary. (B) Alignment of the cysteine-rich C-terminal sequence of human AGRP and mouse agouti proteins. Amino acids 87–132 of AGRP and 92–131 of agouti are shown. Conserved cysteines are highlighted in yellow, and the Mcr binding triplet, RFF, is shown in red. The pattern of disulfide bonding is indicated by brackets, with linkages 1–3 forming the "core" of the three-dimensional structure, as determined by BOLIN *et al.* (1999), while bonds 4 and 5 appear to present and stabilize the RFF-containing loop. Asterisks below mouse agouti residues Cys_{110}, Ser_{112}, Cys_{115}, and Arg_{118} correspond to the sites of mutations in alleles 20R, 14R, 19R, and 21–22R, respectively.

notype group, with the exception of the severe hypomorphs. Overall, the C-terminal mutations were more devastating than the basic-region mutations, and the signal-peptide lesions were comparatively modest. Exceptions to these general rules are noted, however (a^{1R}, a^{3R}, a^{10R}). Among the putative regulatory mutations, five alleles reflected lower mRNA levels in skin relative to the wild-type controls, although the absolute decrease in mRNA expression did not necessarily correlate with severity of the phenotype (*e.g.*, a^{4R}, a^{5R} *vs.* a^{16R}, a^{17R}). On the basis of variation among the homozygous coding-region mutations and the wild-type controls, mild heterogeneity in genetic backgrounds accounts for no >20% fluctuation in mRNA levels. These data suggest that potentially significant differences in *agouti* transcriptional/translational control are likely to play a major role both temporally and spatially in determining how mutant phenotypes correlate with *agouti* mRNA expression patterns in some of the regulatory alleles. Further analysis using *in situ* hybridization of the skin and hair follicles and perhaps immunolocalization of the agouti protein should clarify the basis for many of the subtle hypomorphic phenotypes.

Visual phenotype analysis: In addition to *agouti* gene

structure and expression patterns, other factors influence the appearance of agouti coat phenotypes. The expression level of wild-type *agouti* is determined not only by the degree of Mcr antagonism *in vivo*, but also by the dosage of partially functional agouti proteins. For example, mice homozygous for any given hypomorphic allele generally exhibited milder coat phenotypes (slightly more pheomelanogenic) than were apparent in mice heterozygous (a^R/a) for the same allele. Factors acting independently of *agouti* also influence agouti coat phenotypes. Chief among these is the effect of age on the spatial distribution of pheomelanin along the dorsal/ventral axis. These age-related changes are most striking between weaning and adulthood (3–12 weeks) and are particularly evident in mice carrying hypomorphic alleles. For example, those in the mild category appear nearly wild type as adults, but have a darker, umbrous dorsum at weaning age. Mice with more severe hypomorphic mutations (severe or umbrous-like as adults) typically exhibit nonagouti fur over the entire dorsum and agouti fur in the ventrum at weaning age. Reduced pheomelanin-banded hairs become apparent in adults on the sides and in the dorsum, depending on the phenotypic category. In contrast, amorphic mutations show black fur in both young and adult mice. For these reasons, we deliberately chose to analyze adult fur phenotypes (and primarily dorsal fur) rather than juvenile phenotypes, as the former were generally more stable and better represented each allele. Investigators in the past have consistently observed that pheomelanin is lost from dorsal fur prior to its loss from ventral fur as one progresses down the *agouti* dominance hierarchy (Silvers 1979). Moreover, this effect is not entirely explained by the differential expression of ventral-specific *agouti* transcripts (Bultman *et al.* 1994; Vrieling *et al.* 1994), as equivalent expression of *agouti* variants in the dorsum and ventrum of transgenic mice consistently generates a more pheomelanic ventrum (Perry *et al.* 1995, 1996; Miltenberger *et al.* 1999). Our observation that the dorsal midline is most affected by pheomelanin loss resulting from *a*-locus mutation further suggests that this is the region in which melanocytes are most susceptible to mild variations in *agouti* activity. One possibility is that hair-bulb melanocytes along the dorsal/ventral axis may express variable densities of Mcrs and/or the mahogany protein on their cell surfaces. The effective threshold concentration of agouti required by the melanocyte to switch from eumelanin to pheomelanin synthesis would be greater or more stringent in the dorsum than in the ventrum. Collectively these observations indicate that, in addition to the quality and quantity of *agouti* gene activity, independent and possibly dynamic factors within the hair follicle microenvironment contribute to agouti coat phenotypes.

Chemical analysis of melanins: The chemical method utilized for directly quantifying pheomelanin and eumelanin content of the fur allowed an objective interpretation of *agouti* loss of function in the various alleles. In general agreement with the visibly scored phenotypes, the amounts of the pheomelanin-specific degradation product AHP steadily declined over an ~10-fold range as one progresses down the allelic series analyzed here. However, because absolute AHP levels were not always in perfect agreement with the perceived severity of some *agouti* mutations, the visual phenotype may be a more sensitive discriminator of agouti activity in these cases than the chemical analysis. Seemingly random variation within a <2-fold range was observed for the eumelanin-derived degradation product PTCA in dorsal fur, indicating that, as anticipated, the primary effect of *agouti* mutation was at the level of pheomelanin, not eumelanin, synthesis. A surprising result from this analysis, however, is that the range of adult *agouti* phenotypes from wild type to jet black actually reflects only a minor change (2.3%) in the total melanin distribution. By converting dorsal fur AHP and PTCA values to pheomelanin and eumelanin content, respectively (Ito and Fujita 1985), dorsal midline fur of wild-type agouti mice contains 97.3% eumelanin and 2.7% pheomelanin. Moderate hypomorphic alleles, such as a^{11R}, contain half as much pheomelanin or 1.4% (and 98.6% eumelanin), and visibly black fur, as in the amorphic allele a^{20R}, contains only 0.4% pheomelanin (and 99.6% eumelanin). The reflective qualities of pheomelanin granules and the manner in which individual hairs overlap along the coat probably augment these small differences in pheomelanin content such that even subtle changes in band width or pigment intensity are maximally exposed and readily detectable by the unaided eye.

Regulatory mutations: Using several levels of molecular analysis, we determined that 11 of the 25 *agouti* alleles (10 hypomorphs, 1 amorph) contained wild-type protein-coding sequence, suggesting that regulatory mutations somewhere in the locus interfere with proper and efficient temporal/spatial expression of the wild-type gene products in these mice. The precise genetic alterations remain unidentified, however, as very little is currently known about the elements that contribute to elaborate transcriptional control within the large *agouti* locus. Five of the noncoding hypomorphs that exhibited moderate (a^{4R}, a^{5R}, a^{6R}) to severe (a^{16R}, a^{17R}) phenotypes expressed reduced levels of *agouti* mRNA in neonatal skin compared to wild-type controls. This finding probably accounts for their hypomorphic status, since a strong correlation has been established previously between the level of steady-state RNA synthesis in dominant *agouti* alleles and the amount of pheomelanin in the coat (Duhl *et al.* 1994; Michaud *et al.* 1994b; Yen *et al.* 1994; Hustad *et al.* 1995; Klebig *et al.* 1995; Zemel *et al.* 1995; Argeson *et al.* 1996; Miltenberger *et al.* 1999). Although, as discussed above, imperfect correlation was observed between the absolute level of *agouti* expression and the severity of phenotypes in some alleles, our data nonetheless suggest that approximately threefold or

greater decrease in *agouti* expression levels are sufficient to induce hypomorphic phenotypes *in vivo*. This finding probably reflects the delicate threshold of agouti activity required for effective Mcr antagonism.

Two hypomorphic alleles for which no DNA alterations were identified (a^{11R}, moderate; a^{15R}, umbrous-like) may represent a different class of regulatory mutation, as these mice expressed wild-type *agouti* message at normal to high levels in neonatal skin. Although the timing of *agouti* expression (day 4) was apparently normal in these mice, mutational alterations in spatial control elements could misdirect *agouti* expression to anomalous cell type(s) in the skin, leading to less optimal diffusion and localization of the wild-type agouti protein. Normally, the agouti protein is expressed by specialized cells in the dermal papillae (Millar *et al.* 1995) and has a limited diffusion distance *in vivo*, as suggested by skin transplantation (Silvers and Russell 1955) and transgenic experiments (Kucera *et al.* 1996). *In situ* hybridization or immunolocalization studies will be needed to determine if *agouti* is indeed mislocalized in the a^{11R} and a^{15R} alleles. Three other hypomorphs (a^{2R}, mild; a^{7R}, moderate; a^{18R}, severe) and the amorphic allele a^{24R} also exhibited no coding alterations and likewise may have acquired devastating lesions in critical regulatory element(s) that either reduce/eliminate *agouti* expression or sufficiently relocate its site of synthesis *in vivo* such that subthreshold levels of functional agouti protein reach hair-bulb melanocytes. As more data become available from mouse genome sequencing efforts, previously uncharacterized regions of the ≥125-kb *agouti* locus should become more amenable to mutation screening, and the lesions in these 11 noncoding alleles more readily identifiable. In the meantime, these alleles will provide a rich mutant resource for future investigation into the poorly understood, yet complex, arena of *agouti* transcriptional control.

Signal peptide mutations: Two hypomorphic mutations (a^{8R}, a^{9R}) with moderate coat phenotypes were found to alter the coding potential of the agouti signal peptide. The a^{8R} allele carries an in-frame deletion of 9 bp that eliminates Phe_{14}-Cys_{16}; the slightly more severe a^{9R} allele contains a single missense mutation (T → A) that substitutes Asp for the conserved Val_3. Requirement for an intact signal peptide *in vivo* has been demonstrated previously (Hustad *et al.* 1995; Perry *et al.* 1996), in keeping with early seminal studies that indicated a paracrine role for *agouti* in pigmentation (Silvers and Russell 1955). Analyses by two neural networks, TargetP (Emanuelsson *et al.* 2000) and SignalP (Nielsen *et al.* 1997), provide clues to the cell biological defects caused by these mutations. Reduced hydrophobic-core length in the a^{8R} signal peptide and the net negative charge at the a^{9R} N terminus may interfere with targeting of the nascent preproteins to the endoplasmic reticulum (ER; TargetP score: wt 0.961, a^{8R} 0.900, a^{9R} 0.955). In addition, reduced efficiency of signal peptide processing at an alternative site (Ala_{22}) in a^{8R} and at the wild-type site (Ser_{22}) in a^{9R} may also play a role (SignalP Y score: wt 0.743, a^{8R} 0.662, a^{9R} 0.708). Although the functional impact of an altered N terminus (ΔHisLeuAla) in the mature a^{8R} protein is not known, reduced ER targeting efficiency/fidelity of the a^{8R} preprotein is probably sufficient to induce a loss-of-function phenotype *in vivo*. Potential ramifications include reduced secretion rate and delayed diffusion of the mature protein to target cells. Because the a^{9R} allele is predicted to generate a wild-type mature protein, these analyses also suggest that reduced quantity, not quality, of mature secreted a^{9R} protein is responsible for reduced agouti function in these mice.

Basic region mutations: All coding-region mutations were expressed at approximately wild-type levels, with the exception of the hypomorphic allele a^{10R}. This allele contained a single base change at the splice-acceptor site in exon 4, prompting usage of an internal AG in the fourth exon that is apparently less efficient than the wild-type site. Abnormal splicing in a^{10R} provides an in-frame message for translation and simultaneously deletes two lysine residues ($Lys_{76}Lys_{77}$) in the basic domain. Although the approximately threefold reduction in mRNA levels may contribute to the mutant phenotype in a^{10R}, deletion of the two basic residues is probably of greater significance, since the regulatory mutations, such as a^{4R} and a^{5R}, exhibit greater reductions in mRNA levels yet display a less severe coat phenotype.

The central basic domain of agouti is highly conserved and important for activity *in vivo*, yet its precise biological role is poorly defined (Perry *et al.* 1996; Miltenberger *et al.* 1999). More than one-half of the 29 aa in this domain are basic and often arranged in pairs, suggesting that endoproteolytic processing may generate smaller functional peptides *in vivo*. Western analysis of agouti in mouse tissues has since eliminated this early hypothesis (Ollmann and Barsh 1999), leaving alternative models, such as the following: (1) interaction with mahogany and/or mahoganoid (Dinulescu and Cone 2000; Gunn and Barsh 2000; He *et al.* 2001); (2) facilitation of intracellular trafficking/biogenesis of the mature agouti protein; (3) promoting diffusion to cellular targets following secretion; and/or (4) direct interaction with Mc1r (Virador *et al.* 2000). A common theme that emerged from characterizing the three point mutations (a^{3R}, a^{12R}, a^{13R}) and one small deletion (a^{10R}) that map to the agouti basic region is that net charge may be important for biological activity. In wild-type agouti, 16 basic (12 Lys, 4 Arg) and 2 acidic (Glu) residues generate a net +14 charge over the middle of the protein. Deletion of $Lys_{76}Lys_{77}$ in a^{10R} reduces the net positive charge to +12, generating a moderate dark-agouti phenotype. A single base change (G → A) in the mild allele, a^{3R}, converts 1 of the 2 acidic residues (Glu_{66}) to a basic aa (Lys), thereby increasing the net charge to +16. The second acidic aa (Glu_{68}), which is absolutely conserved in all homologs, was also modified to Lys in

two more severe alleles, a^{12R} (CG → AA) and a^{13R} (G → A). Comparison of the phenotypes of a^{3R} (mild) *vs.* a^{12R} and a^{13R} (umbrous-like) suggests that the position of charged residues, rather than simply the net charge, influences agouti activity. Although the biological role of the basic domain remains unclear, the four mutations identified here could serve as useful tools for testing various hypotheses. Potential protein-protein interactions could be directly addressed *in vivo* by epistasis or double-mutant studies. In addition, although wild-type agouti is not processed beyond the signal peptide *in vivo*, the basic region mutations identified here could introduce new cleavage site(s) for proteolytic convertases, thereby yielding aberrantly processed forms of agouti *in vivo*.

C-terminal mutations: The final group of coding-region mutations maps to the C terminus of agouti, with most alleles being null except for a^{1R} and a^{14R}. Spacing of the 10 cysteine residues in the C terminus is absolutely conserved in all *agouti* homologs, as are 9 out of the 10 cysteines in the C terminus of the agouti-related protein (AGRP, Figure 5B) that naturally antagonizes Mc3r and Mc4r in the central nervous system (Huszar *et al.* 1997; Shutter *et al.* 1997). This arrangement of cysteines bears resemblance to that of the disulfide-bonded ω-conotoxins and ω-agatoxins (Olivera *et al.* 1994; Pallaghy *et al.* 1994), suggesting that agouti and AGRP fold into an "inhibitor cysteine-knot" motif that presents the conserved residues $Arg_{116}Phe_{117}Phe_{118}$ (Figure 5B) that mediate direct interaction with Mcrs (Kiefer *et al.* 1998). Indeed, both mouse agouti (Willard *et al.* 1995) and AGRP (Bures *et al.* 1998) disulfide bond in the same pattern found in the ω-agatoxins; however, agouti and AGRP both contain an additional disulfide linkage (disulfide 5 in Figure 5B). Based on NMR studies of a chemically synthesized and biologically active form of AGRP, three disulfide bridges (bonds 1–3 in Figure 5B corresponding to Cys_{92}-Cys_{107}, Cys_{99}-Cys_{113}, and Cys_{106}-Cys_{124} in mouse agouti) build the core of the C-terminal domain structure (Bolin *et al.* 1999). These core linkages are located at the base of the structure to anchor the bottoms of loops that present Mcr-interacting motifs. The fourth disulfide linkage in AGRP, which is analogous to Cys_{115}-Cys_{122} in mouse agouti (disulfide 4 in Figure 5B), appears to stabilize the relatively rigid "active loop" that contains the $Arg_{116}Phe_{117}Phe_{118}$ binding determinants. The fifth disulfide (Cys_{110}-Cys_{131} in mouse agouti; bond 5 in Figure 5B), which is not present in the ω-agatoxins, is highly reducible *in vitro* (Bures *et al.* 1998), suggesting that it may be more exposed on the exterior of the three-dimensional structure.

Using transgenic mice, Perry *et al.* (1996) determined that individual cysteines are indeed critical for the activity of mouse agouti *in vivo*. Individual cysteines were changed to serine, the mutant cDNAs were expressed under the control of the β-actin promoter, and founder mice were assayed for yellow-pigmented fur and maturity-onset obesity (Perry *et al.* 1996). Mutation of four of the five disulfide bonding pairs (Cys_{92}-Cys_{107}, Cys_{99}-Cys_{113}, Cys_{106}-Cys_{124}, and Cys_{115}-Cys_{122}; bonds 1–4 in Figure 5B) completely abolished activity. In contrast, mutation at Cys_{110} or Cys_{131}, which together form the fifth disulfide connection, resulted in partial loss of function, particularly a tendency toward black pigmentation in the dorsum and yellow pigmentation in the ventrum (Perry *et al.* 1996). Interestingly, this disulfide bond, which has no analog in the ω-agatoxins, forms the most flexible peptide loop (Bolin *et al.* 1999) and was found to be more labile to reduction *in vitro* (Bures *et al.* 1998). Collectively, the *in vitro* and *in vivo* data suggest that the loop formed by Cys_{110}-Cys_{131} (disulfide 5 in Figure 5B) probably does not form the core structure of the agouti C terminus as originally suggested by Bolin *et al.* (1999), but instead serves a secondary role such as stabilizing or facilitating presentation of the Arg_{116}-$Phe_{117}Phe_{118}$-containing loop.

In the present investigations, two alleles were found to disrupt C-terminal cysteine residues (a^{20R} Cys_{110} → stop; a^{19R} Cys_{115} → Ser); however, only the former was a true null. In a^{20R}, a C → A change at Cys_{110} introduces a stop codon, indicating no translation of the Mcr-binding determinants and elimination of three disulfide bonds, hence the null phenotype. The T → A mutation in a^{19R}, however, results in a nearly null phenotype in which residual agouti activity is detectable as pheomelanin around the mammae and perineum, but not on or behind the ears, thus placing this allele between *nonagouti* and true nulls in the *agouti* dominance hierarchy. The a^{19R} mutation prevents formation of the fourth disulfide pair (Cys_{115}-Cys_{122}) that in AGRP stabilizes the Arg_{116} $Phe_{117}Phe_{118}$-containing loop, but does not actually form the core of the C-terminal structure (Bolin *et al.* 1999). The nearly null phenotype of a^{19R} mice is consistent with these structural data. Furthermore, this phenotype suggests that the ventral hair follicle microenvironment around the mammae and perineum is extremely sensitive to minimal levels of agouti activity. Surprisingly, however, this allele is analogous to the Cys_{115}Ser mutation studied by Perry *et al.* (1996) in which the transgenic mice exhibited no agouti activity whatsoever. Discrepancy between the phenotype of a^{19R} mice with the findings of Perry *et al.* (1996) may be explained by their use of transgenic founder animals that may not uniformly express the transgene in all cell types.

Two other null mutations were shown to affect the putative Mcr-binding determinant at Phe_{118} (a^{21R} Phe_{118}-Ala_{121}; a^{22R} Phe_{118} → Ser). The a^{21R} mutation deletes the last aa in the triplet binding determinant for Mcrs, in addition to two other C-terminal aa, thus inducing a reading-frame shift that eliminates the disulfide bonding partners for three of the five disulfide connections. Because the a^{22R} allele is a single missense mutation at Phe_{118}, it provides the first direct evidence that this aromatic residue is indeed critical for agouti activity

in vivo. An alternative explanation for the eumelanic phenotype of a^{22R}, in particular, is that the point mutation of Phe_{118} may convert agouti into a potent agonist of Mc1r (Ollmann *et al.* 1998), rather than into a crippled antagonist. Although our genetic tests show no indication that a^{22R} behaves differently from other jet-black agouti mutations analyzed here (*i.e.*, A/a^{22R} looks identical to other null alleles balanced with *A* or A^{w}), this hypothesis could be formally addressed by direct Mc1r binding studies with labeled mutant agouti protein *in vitro*.

Considering the complex structural constraints guiding the successful folding needed for building a functional agouti C terminus, it is not surprising that deletions that alter the entire coding potential of this region also induced amorphic phenotypes. In a^{23R}, a 3-bp deletion/2-bp insertion event at the end of exon 2 introduces six missense aa at positions 49–54, followed by premature termination just inside exon 3, thereby eliminating the entire basic and C-terminal domains. A 359-bp deletion was identified in a^{25R}, encompassing all of exon 3 and resulting in direct splicing of exon 2 to exon 4. A similar effect on the *agouti* mRNA has been described for the a^{5MNURg} allele that resulted from deletion of a larger genomic fragment (~5 kb) in this vicinity (Bultman *et al.* 1991).

Surprisingly, the mildest allele characterized in this study also carries a lesion within the agouti C terminus. A single base change at the stop codon (G → T) in a^{1R} results in an additional 27 aa at the very C terminus of an otherwise normal agouti protein, producing apparently little impact on normal protein folding or on the interactions with Mc1r. This finding is consistent with the observation that the C-terminal end of AGRP exhibits very little structure in solution and is not involved in stabilizing or presenting the $Arg_{116}Phe_{117}Phe_{118}$-containing loop (Bolin *et al.* 1999). In contrast, the other hypomorphic mutation in the agouti C terminus (a^{14R}, T → C) converts Ser_{112} → Pro and induces a more severe, umbrous-like phenotype. Due to the helix-disrupting or turn potential of prolines and the proximity of this mutation to the closely spaced, conserved cysteines (Figure 5B), this mutation may alter the pairing of one or more disulfide bonds. Furthermore, lower rates of agouti secretion could occur in a^{14R} due to ER retention and retrograde translocation of improperly folded proteins to the proteasome (Wiertz *et al.* 1996).

Toxicology: In addition to new insights into the structure and function of *agouti*, analysis of these multiple *a*-locus alleles provides useful toxicological data for better understanding the molecular mechanisms by which the various mutagens impact the mammalian germline. Analysis of SLT mutations at seven loci in the mouse have shown that the germ-cell stage is the chief determinant of whether mutational lesions are multi or single locus (Russell 1991, 2002). The proportion of the latter type, which is generally compatible with homozygous viability, is considerably higher for mutations induced in spermatogonia than for those induced in postspermatogonial stages or oocytes. For the present investigations, only homozygous viable *a*-locus alleles were selected, and thus it is not surprising that 21 of the 23 (91%) that originated in mutagenized germ cells (a^{4R} and a^{22R} were spontaneous) were induced in spermatogonia. The remaining 2 were induced by X rays, 1 in oocytes (a^{2R}) and 1 in early spermatids (a^{8R}).

Overall, differences were observed among the various treatment groups in the ratio of coding *vs.* regulatory mutations. Of eight mutations induced by chemicals in spermatogonia, six (86%) were coding-region alleles, and these were point mutations, not deletions. By contrast, fewer than one-half (6 out of 15 or 40%) of mutations induced by radiations in spermatogonia were coding-region alleles, with 3 of the 6 being deletions. Of the two mutations not induced in spermatogonial stages, one occurred in the protein-coding region. Other information derived from SLT-induced mutations (Russell 2002) indicated that mutational lesions induced in postspermatogonial stages are more extensive than those induced in spermatogonia and that, among mutations induced in spermatogonia, those induced by radiations are more extensive than those induced by chemicals. The proportion of *a*-locus alleles that are not in the coding region follows the same relative order. It might therefore be suggested that these alleles may turn out to include a relatively small percentage of single-base-pair changes.

Of the five mutations generated with *N*-ethyl-*N*-nitrosourea (ENU) in spermatogonial stem cells, only one was an uncharacterized regulatory mutation (a^{15R}), and four were single-base substitutions. The A/T → T/A transversions in a^{9R} and a^{19R} and the A/T → G/C transition in a^{14R} typify ~80% of the ENU-induced mouse germ-cell mutations identified in other studies (Noveroske *et al.* 2000). The fourth ENU mutation (a^{20R}), a G/C → A/T transversion, is a type that had been found only rarely in the past. The *N*-methyl-*N*-nitrosourea (MNU)-induced allele, a^{3R}, was shown to carry a G/C → A/T transition, as is characteristic of this methylating agent in mouse germ cells (Vogel and Natarajan 1995; Favor 1999). Although the mechanism by which ethylene oxide induces mutations in the mammalian germline remains unclear (Dellarco *et al.* 1990), the A/T → T/A mutation identified in a^{10R} is consistent with N-alkylation damage (Vogel and Natarajan 1995). Finally, synthetic fuel induced an unidentified regulatory mutation in a^{7R}; however, this lesion could be a deletion like the previously characterized $Bmp5^{3SYNg}$ allele that was also generated with synthetic fuel in SLTs (Marker *et al.* 1997).

Of the seven loci screened in SLTs, the *a* locus is one of the two least mutable for either radiation or chemical treatment, representing only 0–7% of all mutants recovered (Russell 2002). Spontaneous mutations arising in mitotic stages of gametogenesis are also extremely

rare at the *a* locus. In fact, among the 66 such mutations reported for SLTs by three laboratories, none has been at the *a* locus (Russell and Russell 1996). On the other hand, among spontaneous mutations arising during the perigametic interval (Russell and Russell 1996; Russell 1999) over one-third involved the *a* locus. Two of these perigametic *a*-locus mutations were analyzed in the present study. One (a^{22R}) was determined to be a single-base-pair change of a type (A/T → G/C) that has been reported to be common after ENU mutagenesis (see above); the other (a^{4R}) was found to be outside the coding regions, and the DNA alteration remains to be identified.

Concluding remarks: The extensive and diverse set of recessive, homozygous-viable, and intragenic mutations in the *agouti* gene generated in SLTs at ORNL has permitted us to perform detailed structure/function analysis of the agouti protein. As was previously shown for other SLT loci (*Tyrp1*, Sarangarajan *et al.* 2000; *Tyr*, Yokoyama *et al.* 1990 and Rinchik *et al.* 1993; *Myo5a*, Huang *et al.* 1998a,b; *Bmp*, Marker *et al.* 1997; and *Ednrb*, Shin *et al.* 1997), an allelic series of intragenic mutations that alter (but do not necessarily eliminate) a protein or its regulation is an invaluable tool in discovering the scope of *in vivo* biological functions of a gene. The community-wide effort to generate ENU-induced mutant alleles of genes throughout the genome, both by phenotype-driven and gene-driven approaches (Justice *et al.* 1999; Rinchik 2000; Brown and Balling 2001), underscores the usefulness of these tools and will provide important reagents for deciphering gene functions, interactions, and regulatory networks.

We thank Pat Hunsicker, Gene Barker, Bob Olszewski, Jean Bangham, and all other animal caretakers past and present at ORNL. We also thank Anne Chang for technical assistance; Dr. Peter Hoyt for helping to photograph mice; and Dr. Richard Mural, Dr. Loren Houser, Melissa York, and Shen Lu at the ORNL sequencing facility. Critical review of the manuscript was graciously provided by Drs. Eugene Rinchik, Dabney Johnson, and Barry Bruce. Research was sponsored jointly by the National Institute of Environmental Health Sciences, under Interagency Agreement no. 1-Y01-ES-50318-00 (to L.B.R.); the Office of Health and Environmental Research, U.S. Department of Energy, under contract DE-AC05-960R22464 with Lockheed Martin Energy Systems, Inc. (to R.P.W.); and the Office of Biological and Environmental Research, U.S. Department of Energy, under contract DE-AC05-00OR22725 with UT-Battelle, LLC (to E.J.M.). Research was also supported by an Alexander Hollaender Distinguished Postdoctoral Fellowship (to R.J.M.), sponsored by the Department of Energy, Office of Health and Environmental Research, and administered by the Oak Ridge Institute for Science and Education; and by Grants-in-Aid for Scientific Research (10670812 and 1270844) to K.W. and S.I., sponsored by the Ministry of Education, Science, and Culture of Japan.

LITERATURE CITED

Argeson, A. C., K. K. Nelson and L. D. Siracusa, 1996 Molecular basis of the pleiotropic phenotype of mice carrying the *hypervariable yellow* (A^{hvy}) mutation at the *agouti* locus. Genetics **142:** 557–567.

Ausubel, F. M., R. Brent, R. E. Kingston, D. D. Moore, J. G. Seidman *et al.* (Editors), 1989 *Current Protocols in Molecular Biology*. John Wiley & Sons, New York.

Blobel, G., and B. Dobberstein, 1975 Transfer of proteins across membranes. I. Presence of proteolytically processed and unprocessed nascent immunoglobulin light chains on membrane-bound ribosomes of murine myeloma. J. Cell Biol. **67:** 835–851.

Bolin, K. A., D. J. Anderson, J. A. Trulson, D. A. Thompson, J. Wilken *et al.*, 1999 NMR structure of a minimized human agouti related protein prepared by total chemical synthesis. FEBS Lett. **451:** 125–131.

Brown, S. D., and R. Balling, 2001 Systematic approaches to mouse mutagenesis. Curr. Opin. Genet. Dev. **11:** 268–273.

Bultman, S. J., L. B. Russell, G. A. Gutierrez-Espeleta and R. P. Woychik, 1991 Molecular characterization of a region of DNA associated with mutations at the *agouti* locus in the mouse. Proc. Natl. Acad. Sci. USA **88:** 8062–8066.

Bultman, S. J., E. J. Michaud and R. P. Woychik, 1992 Molecular characterization of the mouse *agouti* locus. Cell **71:** 1195–1204.

Bultman, S. J., M. L. Klebig, E. J. Michaud, H. O. Sweet, M. T. Davisson *et al.*, 1994 Molecular analysis of reverse mutations from *nonagouti* (*a*) to *black-and-tan* (a^t) and *white-bellied agouti* (A^w) reveals alternative forms of agouti transcripts. Genes Dev. **8:** 481–490.

Bures, E. J., J. O. Hui, Y. Young, D. T. Chow, V. Katta *et al.*, 1998 Determination of disulfide structure in agouti-related protein (AGRP) by stepwise reduction and alkylation. Biochemistry **37:** 12172–12177.

Chen, Y., D. M. Duhl and G. S. Barsh, 1996 Opposite orientations of an inverted duplication and allelic variation at the mouse *agouti* locus. Genetics **144:** 265–277.

Church, G. M., and W. Gilbert, 1984 Genomic sequencing. Proc. Natl. Acad. Sci. USA **81:** 1991–1995.

Dellarco, V. L., W. M. Generoso, G. A. Sega, J. R. Fowle, 3rd and D. Jacobson-Kram, 1990 Review of the mutagenicity of ethylene oxide. Environ. Mol. Mutagen. **16:** 85–103.

Dinulescu, D. M., and R. D. Cone, 2000 Agouti and agouti-related protein: analogies and contrasts. J. Biol. Chem. **275:** 6695–6698.

Duhl, D. M., H. Vrieling, K. A. Miller, G. L. Wolff and G. S. Barsh, 1994 Neomorphic *agouti* mutations in obese yellow mice. Nat. Genet. **8:** 59–65.

Emanuelsson, O., H. Nielsen, S. Brunak and G. von Heijne, 2000 Predicting subcellular localization of proteins based on their N-terminal amino acid sequence. J. Mol. Biol. **300:** 1005–1016.

Favor, J., 1999 Mechanisms of mutation induction in germ cells of the mouse as assessed by the specific locus test. Mutat. Res. **428:** 227–236.

Gunn, T. M., and G. S. Barsh, 2000 Mahogany/attractin: en route from phenotype to function. Trends Cardiovasc. Med. **10:** 76–81.

Gunn, T. M., K. A. Miller, L. He, R. W. Hyman, R. W. Davis *et al.*, 1999 The mouse *mahogany* locus encodes a transmembrane form of human attractin. Nature **398:** 152–156.

Gunn, T. M., T. Inui, K. Kitada, S. Ito, K. Wakamatsu *et al.*, 2001 Molecular and phenotypic analysis of attractin mutant mice. Genetics **158:** 1683–1695.

He, L., T. M. Gunn, D. M. Bouley, X. Y. Lu, S. J. Watson *et al.*, 2001 A biochemical function for attractin in agouti-induced pigmentation and obesity. Nat. Genet. **27:** 40–47.

Huang, J. D., M. J. Cope, V. Mermall, M. C. Strobel, J. Kendrick-Jones *et al.*, 1998a Molecular genetic dissection of mouse unconventional myosin-VA: head region mutations. Genetics **148:** 1951–1961.

Huang, J. D., V. Mermall, M. C. Strobel, L. B. Russell, M. S. Mooseker *et al.*, 1998b Molecular genetic dissection of mouse unconventional myosin-VA: tail region mutations. Genetics **148:** 1963–1972.

Hustad, C. M., W. L. Perry, L. D. Siracusa, C. Rasberry, L. Cobb *et al.*, 1995 Molecular genetic characterization of six recessive viable alleles of the mouse *agouti* locus. Genetics **140:** 255–265.

Huszar, D., C. A. Lynch, V. Fairchild-Huntress, J. H. Dunmore, Q. Fang *et al.*, 1997 Targeted disruption of the melanocortin-4 receptor results in obesity in mice. Cell **88:** 131–141.

Ito, S., 1998 Advances in chemical analysis of melanins, pp. 439–450 in *The Pigmentary System*, edited by J. J. Nordlund, R. E. Boissy,

V. J. Hearing, R. A. King and J.-P. Ortonne. Oxford University Press, New York.

Ito, S., and K. Fujita, 1985 Microanalysis of eumelanin and pheomelanin in hair and melanomas by chemical degradation and liquid chromatography. Anal. Biochem. **144:** 527–536.

Justice, M. J., J. K. Noveroske, J. S. Weber, B. Zheng and A. Bradley, 1999 Mouse ENU mutagenesis. Hum. Mol. Genet. **8:** 1955–1963.

Kiefer, L. L., O. R. Ittoop, K. Bunce, A. T. Truesdale, D. H. Willard *et al.*, 1997 Mutations in the carboxyl terminus of the agouti protein decrease agouti inhibition of ligand binding to the melanocortin receptors. Biochemistry **36:** 2084–2090.

Kiefer, L. L., J. M. Veal, K. G. Mountjoy and W. O. Wilkison, 1998 Melanocortin receptor binding determinants in the agouti protein. Biochemistry **37:** 991–997.

Klebig, M. L., J. E. Wilkinson, J. G. Geisler and R. P. Woychik, 1995 Ectopic expression of the *agouti* gene in transgenic mice causes obesity, features of type II diabetes, and yellow fur. Proc. Natl. Acad. Sci. USA **92:** 4728–4732.

Kucera, G. T., D. M. Bortner and M. P. Rosenberg, 1996 Overexpression of an Agouti cDNA in the skin of transgenic mice recapitulates dominant coat color phenotypes of spontaneous mutants. Dev. Biol. **173:** 162–173.

Kwon, H. Y., S. J. Bultman, C. Loffler, W. J. Chen, P. J. Furdon *et al.*, 1994 Molecular structure and chromosomal mapping of the human homolog of the *agouti* gene. Proc. Natl. Acad. Sci. USA **91:** 9760–9764.

Lamoreux, M. L., K. Wakamatsu and S. Ito, 2001 Interaction of major coat color gene functions in mice as studied by chemical analysis of eumelanin and pheomelanin. Pigment Cell Res. **14:** 23–31.

Leeb, T., A. Doppe, B. Kriegesmann and B. Brenig, 2000 Genomic structure and nucleotide polymorphisms of the porcine *agouti signalling protein* gene (ASIP). Anim. Genet. **31:** 335–336.

Lu, D., D. Willard, I. R. Patel, S. Kadwell, L. Overton *et al.*, 1994 Agouti protein is an antagonist of the melanocyte-stimulating-hormone receptor. Nature **371:** 799–802.

Marker, P. C., K. Seung, A. E. Bland, L. B. Russell and D. M. Kingsley, 1997 Spectrum of Bmp5 mutations from germline mutagenesis experiments in mice. Genetics **145:** 435–443.

Matsunaga, N., V. Virador, C. Santis, W. D. Vieira, M. Furumura *et al.*, 2000 *In situ* localization of agouti signal protein in murine skin using immunohistochemistry with an ASP-specific antibody. Biochem. Biophys. Res. Commun. **270:** 176–182.

Michaud, E. J., S. J. Bultman, M. L. Klebig, M. J. van Vugt, L. J. Stubbs *et al.*, 1994a A molecular model for the genetic and phenotypic characteristics of the mouse *lethal yellow* (A^y) mutation. Proc. Natl. Acad. Sci. USA **91:** 2562–2566.

Michaud, E. J., M. J. van Vugt, S. J. Bultman, H. O. Sweet, M. T. Davisson *et al.*, 1994b Differential expression of a new dominant *agouti* allele (A^{iapy}) is correlated with methylation state and is influenced by parental lineage. Genes Dev. **8:** 1463–1472.

Millar, S. E., M. W. Miller, M. E. Stevens and G. S. Barsh, 1995 Expression and transgenic studies of the mouse *agouti* gene provide insight into the mechanisms by which mammalian coat color patterns are generated. Development **121:** 3223–3232.

Miller, K. A., T. M. Gunn, M. M. Carrasquillo, M. L. Lamoreux, D. B. Galbraith *et al.*, 1997 Genetic studies of the mouse mutations *mahogany* and *mahoganoid*. Genetics **146:** 1407–1415.

Miller, M. W., D. M. Duhl, B. M. Winkes, F. Arredondo-Vega, P. J. Saxon *et al.*, 1994 The mouse lethal nonagouti (a^x) mutation deletes the S-adenosylhomocysteine hydrolase (*Ahcy*) gene. EMBO J. **13:** 1806–1816.

Miltenberger, R. J., R. L. Mynatt, B. D. Bruce, W. O. Wilkison, R. P. Woychik *et al.*, 1999 An agouti mutation lacking the basic domain induces yellow pigmentation but not obesity in transgenic mice. Proc. Natl. Acad. Sci. USA **96:** 8579–8584.

Nagle, D. L., S. H. McGrail, J. Vitale, E. A. Woolf, B. J. Dussault, Jr. *et al.*, 1999 The mahogany protein is a receptor involved in suppression of obesity. Nature **398:** 148–152.

Nielsen, H., J. Engelbrecht, S. Brunak and G. von Heijne, 1997 Identification of prokaryotic and eukaryotic signal peptides and prediction of their cleavage sites. Protein Eng. **10:** 1–6.

Noveroske, J. K., J. S. Weber and M. J. Justice, 2000 The mutagenic action of N-ethyl-N-nitrosourea in the mouse. Mamm. Genome **11:** 478–483.

Oakberg, E. F., 1984 Germ cell toxicity: significance in genetic and fertility effects of radiation and chemicals. Environ. Sci. Res. **31:** 549–590.

Olivera, B. M., G. P. Miljanich, J. Ramachandran and M. E. Adams, 1994 Calcium channel diversity and neurotransmitter release. Annu. Rev. Biochem. **63:** 823–867.

Ollmann, M. M., and G. S. Barsh, 1999 Down-regulation of melanocortin receptor signaling mediated by the amino terminus of Agouti protein in Xenopus melanophores. J. Biol. Chem. **274:** 15837–15846.

Ollmann, M. M., B. D. Wilson, Y. K. Yang, J. A. Kerns, Y. Chen *et al.*, 1997 Antagonism of central melanocortin receptors *in vitro* and *in vivo* by agouti-related protein. Science **278:** 135–138. [erratum: Science **281**(5383): 1615].

Ollmann, M. M., M. L. Lamoreux, B. D. Wilson and G. S. Barsh, 1998 Interaction of Agouti protein with the melanocortin 1 receptor *in vitro* and *in vivo*. Genes Dev. **12:** 316–330.

Ozeki, H., S. Ito, K. Wakamatsu and T. Hirobe, 1995 Chemical characterization of hair melanins in various coat-color mutants of mice. J. Invest. Dermatol. **105:** 361–366.

Pallaghy, P. K., K. J. Nielsen, D. J. Craik and R. S. Norton, 1994 A common structural motif incorporating a cystine knot and a triple-stranded beta-sheet in toxic and inhibitory polypeptides. Protein Sci. **3:** 1833–1839.

Perry, W. L., C. M. Hustad, D. A. Swing, N. A. Jenkins and N. G. Copeland, 1995 A transgenic mouse assay for agouti protein activity. Genetics **140:** 267–274.

Perry, W. L., T. Nakamura, D. A. Swing, L. Secrest, B. Eagleson *et al.*, 1996 Coupled site-directed mutagenesis/transgenesis identifies important functional domains of the mouse agouti protein. Genetics **144:** 255–264.

Rinchik, E. M., 2000 Developing genetic reagents to facilitate recovery, analysis, and maintenance of mouse mutations. Mamm. Genome **11:** 489–499.

Rinchik, E. M., J. P. Stoye, W. N. Frankel, J. Coffin, B. S. Kwon *et al.*, 1993 Molecular analysis of viable spontaneous and radiation-induced albino (*c*)-locus mutations in the mouse. Mutat. Res. **286:** 199–207.

Russell, L. B., 1991 Factors that affect the molecular nature of germ-line mutations recovered in the mouse specific-locus test. Environ. Mol. Mutagen. **18:** 298–302.

Russell, L. B., 1999 Significance of the perigametic interval as a major source of spontaneous mutations that result in mosaics. Environ. Mol. Mutagen. **34:** 16–23.

Russell, L. B., 2002 Effects of male germ-cell stage on the frequency, nature, and spectrum of induced specific-locus mutations in the mouse. Genetica (in press).

Russell, L. B., and W. L. Russell, 1996 Spontaneous mutations recovered as mosaics in the mouse specific-locus test. Proc. Natl. Acad. Sci. USA **93:** 13072–13077. (erratum: Proc. Natl. Acad. Sci. USA **94:** 4233).

Russell, W. L., 1951 X-ray induced mutations in mice. Cold Spring Harbor Symp. Quant. Biol. **16:** 327–336.

Sambrook, J., E. F. Fritsch and T. Maniatis, 1989 *Molecular Cloning: A Laboratory Manual*. Cold Spring Harbor Laboratory Press, Plainview, NY.

Sarangarajan, R., Y. Zhao, G. Babcock, J. Cornelius, M. L. Lamoreux *et al.*, 2000 Mutant alleles at the *brown* locus encoding tyrosinase-related protein-1 (TRP-1) affect proliferation of mouse melanocytes in culture. Pigment Cell Res. **13:** 337–344.

Shin, M. K., L. B. Russell and S. M. Tilghman, 1997 Molecular characterization of four induced alleles at the *Ednrb* locus. Proc. Natl. Acad. Sci. USA **94:** 13105–13110.

Shutter, J. R., M. Graham, A. C. Kinsey, S. Scully, R. Luthy *et al.*, 1997 Hypothalamic expression of ART, a novel gene related to agouti, is up-regulated in obese and diabetic mutant mice. Genes Dev. **11:** 593–602.

Silvers, W. K., 1979 *The Coat Colors of Mice: A Model for Mammalian Gene Action and Interaction*. Springer-Verlag, New York.

Silvers, W. K., and E. S. Russell, 1955 An experimental approach to action of genes at the *agouti* locus in the mouse. J. Exp. Zool. **130:** 199–220.

Virador, V. M., C. Santis, M. Furumura, H. Kalbacher and V. J. Hearing, 2000 Bioactive motifs of agouti signal protein. Exp. Cell Res. **259:** 54–63.

Vogel, E. W., and A. T. Natarajan, 1995 DNA damage and repair in somatic and germ cells *in vivo*. Mutat. Res. **330:** 183–208.

Vrieling, H., D. M. Duhl, S. E. Millar, K. A. Miller and G. S. Barsh, 1994 Differences in dorsal and ventral pigmentation result from regional expression of the mouse *agouti* gene. Proc. Natl. Acad. Sci. USA **91:** 5667–5671.

Wiertz, E. J. H. J., D. Tortorella, M. Bogyo, J. Yu, W. Mothes *et al.*, 1996 Sec61-mediated transfer of a membrane protein from the endoplasmic reticulum to the proteasome for destruction. Nature **384:** 432–438.

Willard, D. H., W. Bodnar, C. Harris, L. Kiefer, J. S. Nichols *et al.*, 1995 Agouti structure and function: characterization of a potent alpha-melanocyte stimulating hormone receptor antagonist. Biochemistry **34:** 12341–12346.

Yen, T. T., A. M. Gill, L. G. Frigeri, G. S. Barsh and G. L. Wolff, 1994 Obesity, diabetes, and neoplasia in yellow A^{vy}/- mice: ectopic expression of the agouti gene. FASEB J. **8:** 479–488.

Yokoyama, T., D. W. Silversides, K. G. Waymire, B. S. Kwon, T. Takeuchi *et al.*, 1990 Conserved cysteine to serine mutation in tyrosinase is responsible for the classical *albino* mutation in laboratory mice. Nucleic Acids Res. **18:** 7293–7298.

Zemel, M. B., J. H. Kim, R. P. Woychik, E. J. Michaud, S. H. Kadwell *et al.*, 1995 Agouti regulation of intracellular calcium: role in the insulin resistance of viable yellow mice. Proc. Natl. Acad. Sci. USA **92:** 4733–4737.

Communicating editor: N. A. Jenkins